Spatial Averages of Coverage Characteristics in Large CDMA Networks

François Baccelli, Bartlomiej Blaszczyszyn, Florent Tournois

INRIA

INSTITUT NATIONAL DE RECHERCHE EN INFORMATIQUE ET EN AUTOMATIQUE

Spatial Averages of Coverage Characteristics in Large CDMA Networks

François Baccelli — Bartłomiej Błaszczyszyn — Florent Tournois

N° 4196

Juin 2001

THÈME 1

ISSN 0249-6399 ISRN INRIA/RR--4196--FR+ENG

INRIA
ROCQUENCOURT

Spatial Averages of Coverage Characteristics in Large CDMA Networks

François Baccelli* , Bartłomiej Błaszczyszyn† , Florent Tournois‡

Thème 1 — Réseaux et systèmes
Projet TREC

Rapport de recherche n° 4196 — Juin 2001 — 32 pages

Abstract: The aim of the present paper is to show that stochastic geometry provides an efficient computational framework allowing one to predict geometrical characteristics of large CDMA networks such as coverage or soft-handoff level. The general idea consists in representing the location of antennas and/or mobile stations as realizations of stochastic point processes in the plane within a simple parametric class, which takes into account the irregularities of antenna/mobile patterns in a statistical way. This approach leads to new formulas and simulation schemes allowing one to compute/estimate the spatial averages of these local characteristics in function of the model parameters (density of antennas or mobiles, law of emission power, fading law etc.) and to perform various parametric optimizations.

Key-words: CDMA, stochastic geometry model, exact simulation, Shannon capacity level-sets, handoff zones, coverage probability, mean cell area, contact distribution function, parametric optimisation

* ENS/INRIA, 45 rue d'Ulm, 75005 Paris; e-mail: Francois.Baccelli@ens.fr. This research was partially funded by the France Télécom CTI grant N 1 98 E 222 00 41611 01 2 and by the RNRT *Georges* project

† ENS/INRIA & University of Wrocław, 45 rue d'Ulm, 75005 Paris; e-mail: Bartek.Blaszczyszyn@ens.fr. This research was was funded by the France Télécom CTI grant N 1 98 E 222 00 41611 01 2. Additional support also came from KBN grant 2 P03A 049 15

‡ ENS, 45 rue d'Ulm, 75005 Paris; e-mail: Florent.Tournois@ens.fr

Unité de recherche INRIA Rocquencourt
Domaine de Voluceau, Rocquencourt, B.P. 105, 78153 Le Chesnay Cedex (France)
Téléphone : 01 39 63 55 11 - International : +33 1 39 63 55 11 —Fax : (33) 01 39 63 53 30 - International : +33 1 39 63 53 30

Moyennes Spatiales des Caractéristiques de la Couverture dans les Grands Réseaux CDMA

Résumé : La but de cet article est de montrer que la géométrie aléatoire fournit un cadre calculatoire efficace pour la prédiction des caractéristiques géométriques de grands réseaux CDMA, telles que la couverture ou les zones de niveau du *handover*. L'idée générale consiste en une représentation de la localisation des antennes et des mobiles comme réalisations de processus ponctuels aléatoires dans le plan, appartenant à des classes paramétriques simples; ceci permet notamment de prendre en compte les irrégularités et les aléas présents dans les localisations des antennes et des stations mobiles. Cette approche conduit à de nouvelles formules et à de nouveaux schémas de simulation permettant de calculer ou d'estimer les moyennes spatiales de ces caractéristiques en fonction des paramètres du modèle (densité des antennes et des mobiles, loi de la puissance d'émission et de l'évanouissement etc.) et de mettre en oeuvre diverses optimisations paramétriques.

Mots-clés : CDMA, géométrie stochastique, simulation exacte, capacité de Shannon, fonction de niveau, zone de handover, probabilité de couverture, surface moyenne de cellule, distribution de contact, optimisation paramétrique.

1 Introduction

Most of current CDMA analysis is based on a simplified representation of the underlying network geometry:

- Antenna patterns are often represented either by by a finite pattern consisting of one central antenna and its direct neighbors, which is supposed to represent the *typical environment* seen by an antenna, or by an infinite regular pattern of points in the plane, which leads to the classical honeycomb model. Both types of patterns are nevertheless acknowledged to be inadequate, as real patterns in fact contain a very large number of points with no planar regularity at all. This is true not only for networks where antennas are themselves mobile like in ad hoc networks (see e.g. [5]), but also for networks with fixed antennas. For fixed antennas, irregularity stems from the lack of homogeneity of the demographic density; even in the homogeneous case, cost and topographical constraints also lead to quite irregular antenna patterns, particularly so in dense urban areas networks.

- Inter-cell interferences are often represented in a simplified way too which either does not take geometrical data into account at all (e.g. these interferences are included in the so called thermal noise), or uses one of the simplified models alluded to above rather than taking into account the actual location of the antennas causing the interferences.

The lack of adequate representation of geometry is a serious drawback within this setting in that both on the up and the downlink, key local characteristics of CDMA (coverage, soft-handoff level etc.), at a given point of the plane, are based on the Signal to (Interference and) Noise Ratio (SINR, SNR) at this point, which is itself based in an essential way on the local geometry of the network.

The aim of the present paper is to show that stochastic geometry provides an efficient computational framework allowing one to represent these irregular patterns and to analyze their effect on the key local characteristics of CDMA.

The general idea of the present paper consists in representing the location of antennas and that of mobile stations as realizations of stochastic point processes in the plane within a simple parametric class, which takes into account the irregularities mentioned above in a statistical way. A natural versatile parametric model for representing antenna or mobile station point patterns is that of Poisson-Gibbs point processes (see e.g. [15]). The results of the present paper, which is the first step in the development of this methodology, are all based on (possibly non-homogeneous) Poisson point patterns, which are the simplest possible mathematical models within this setting.

This Poisson point process representation is then used together with classical models of propagation and fading, and together with simple power control algorithm models, in order to compute the resulting fluctuations of the key local characteristics of CDMA.

More precisely, this approach leads to formulas and simulation schemes allowing one to compute/estimate the mathematical expectation (and more generally the law) of these local characteristics in function of the model parameters (density of antennas, law of emission power, fading law etc.).

It is important to stress how these mathematical expectations should be interpreted. In the case of a homogeneous Poisson process, the most natural interpretation is in terms of a *planar averaging*. For instance:

- For the probability $p(x)$ that a typical antenna contains a mobile, located at distance x, in its soft-handoff zone, such a planar averaging means the following: pick at random a (large) set of antennas of this irregular pattern; for each antenna within this set, add at random a mobile located at distance x; then $p(x)$ is the empirical frequency with which the added mobile is in the soft-handoff zone of the antenna.

- For the expectation $\mathrm{E}H$ of the soft-handoff level H of a typical mobile: pick at random a large number of locations in the plane; for each of them, add a mobile station there and evaluate its soft-handoff level; then H is the empirical average over this large set of samples.

Non homogeneous networks are of interest in case where the demographic density varies. Let us consider the example of a town where the density depends on the distance to the center only. Then the interpretation is still in terms of *planar averaging*:

- For the probability $p_r(x)$ that the soft-handoff zone of a typical antenna at distance r from the center contains a mobile, located at distance x from the antenna, the empirical averaging would be based on a set of antennas which are approximately at distance r from the center.

- For the expectation $\mathrm{E}H(r)$ of the soft-handoff level $H(r)$ of a typical mobile located at distance r from the center, the empirical averaging would be based on locations picked at random at distance r from the center.

The paper is structured as follows. The basic stochastic geometry model allowing one to capture SNR and some of its most important special cases are described in §2. The CDMA motivations are described in §3. The key performance characteristics are defined in §4. Simulation and analytical results are gathered in §5. This concerns in particular

- Qualitative results on the shape of the cells in function of such parameters as the strength of the attenuation or the interference coefficient;

- The evaluation of the network QoS, e.g. the proportion of the plane where the soft-handoff level is at least k, or the probability that a mobile moving along a random line remains with such a handoff level for more than t;

- Parametric optimization issues, such as maximization of coverage under cost constraints.

The appendix contains two parts: §6.4 summarizes the main formulas and simulation schemes obtained from this approach and which are the basis for the results obtained in §5. §A.4.2 gives the parameters of a list of models that are used to illustrate the results throughout the paper.

2 Generic Stochastic Geometry Model

Let $\Phi = \{(X_i, Z_i)\}$ be a marked point process (for basic definitions on point processes and stochastic geometry, see e.g. [15]) on the 2-dimensional (or more generally d-dimensional) Euclidean space $\mathbb{R}^2$ (resp. $\mathbb{R}^d$), where $\phi = \{X_i\}$ denotes the locations of points, and where the *marks* $Z_i = (A_i, B_i)$ are such that A_i is a matrix with $N_i \leq \infty$ rows and $card(\Phi)$ columns and B_i a column vector of dimension N_i. We assume that the points $\{X_i\}$ are numbered and the

vector of these points is denoted $X = (X_i)$ (the ordering is for instance based on the distance to the origin). As already indicated, all the formulas of the present paper will be based on the assumption that $\{X_i\}$ is the realization of a Poisson point process. However, most of the definitions of this section are generic and do not require such an assumption.

In addition to this marked point process, the model is based on a function $l : \mathbb{R}^2 \to \mathbb{R}^+$, called the attenuation function, which is continuous w.r.t. its arguments; we will assume that $l(x, y) \to 0$ when $|x - y| \to \infty$ (where $|z|$ is the Euclidean norm of z in $\mathbb{R}^2$).

2.1 Individual Cells

We define the *cell* C_0 attached to the point X_0 as the following subset of $\mathbb{R}^2$

$$C_0 = C_0(\Phi) = \left\{ y : \ A_0 L(y, \phi) \geq B_0 \right\}, \tag{2.1}$$

where $L(y, \phi)$ is the column vector with entries $l(y, X_i)$, and where the inequality between two vectors has the usual coordinatewise meaning.

2.2 Special Cases

1. The *Boolean model* (see e.g. [6] or [15])

   $$C_0 = \{y : \ a_0 l(y, X_0) \geq c_0\}$$

   is obtained as the special case where $N_i = 1$, $(A_i)_k = \delta_i(k) a_i$ (δ is the Kronecker function), where a_i and $B_i = c_i$ are non-negative random variables. It is required here that l decreases to 0 with Euclidean distance and that c_i be strictly positive to avoid pathological cases. For the classical Boolean model, the underlying point process should be Poisson and the random variables (a_i, c_i) should be independent and identically distributed (i.i.d.).

2. The *Voronoi tessellation* (see e.g. [10]) is a special case too with $N_i = card(\Phi)$; all entries of A_i and B_i are zero but for $(A_i)_{ji} = 1$, $j \neq i$, and $(A_i)_{jj} = -1$, $j \neq i \in \mathbb{N}$. Here we take $l(x, y) = |x - y|^{-1}$.

3. A more elaborate model (which will be referred to as Model 3 below) with dependent cells, is that introduced in [1]:

   $$C_0 = \{y : \ a_0 S_0 l(y, X_0) \geq b_0 I_\Phi(y) + c_0\},$$

   where $I_\Phi(y)$ is the shot-noise process (see e.g. [21, 13, 8, 7]) of $\{X_i, S_i\}$ at point y for the response function l, namely :

   $$I_\Phi(y) = \sum_{X_i \in \Phi} S_i l(y, X_i) \,. \tag{2.2}$$

   Note it is a special case of (2.1) too with $N_i = 1$, A_i a row vector with kth entry $(A_i)_k = -b_i S_k$ for $k \neq i$ and $(A_i)_i = (a_i - b_i) S_i$, and $B_i = c_i$, with a_i, b_i, c_i, S_i non-negative random variables.

2.3 Extensions

A natural extension to be used in the present paper is that where the matrices A_i and/or the vectors B_i are functions of a parameter $x \in \mathbb{R}^2$.

2.4 Coverage Process

The associated *coverage* process is the union of all cells:

$$\Xi = \Xi(\Phi) = \bigcup_i C_i(\Phi) \tag{2.3}$$

3 Geometry of CDMA Cells

This section summarizes the basic principles of CDMA. We start with the definition of level sets of the Shannon capacity function, which is a natural theoretical basis for the definition of the up and downlinks. We show that these level sets can be seen as a special case of our generic model. We then study more specific features of the uplink and downlink CDMA cells and show that their geometrical properties can be obtained from special instances of our generic model.

3.1 Level-Sets for Shannon Capacity of Planar Vector Channels

In this section we describe models of cells defined by the capacity of certain vector channels where capacity should here be understood in the information theoretic sense.

We consider a vector channel with a K-component input, identified by its baseband representation

$$\mathcal{Y} = \sum_{i=1}^{K} \mathcal{X}_i + \mathcal{Z},$$

where $\mathcal{Y}, \mathcal{X}_i, \mathcal{Z}$ represent the output, the components of the (vector) input and a Gaussian noise respectively.

Let us assume for a moment that there is no spreading; i.e., spreading length $L = 1$, and thus the K components of the channel cannot be distinguished — they simultaneously support the same data stream. The Shannon capacity of this K-user Gaussian multiple-access channel is $\max I(\mathcal{X}_1, \ldots, \mathcal{X}_K; Y)$, where $I(\mathcal{X}_1, \ldots, \mathcal{X}_K; Y)$ is the mutual information between the input and the output, and where the maximum is over all distributions of $\mathcal{X}_i$ with variances bounded from above by some power constraint $P_1, \ldots, P_k$ respectively. It is well known (see. e.g. Chapter 7 in [2]) this maximum is achieved when all $\mathcal{X}_i$ are independent Gaussian random variables, and that the capacity $\mathcal{C}$ of our vector channel is:

$$\mathcal{C} = \frac{1}{2} \log\left(1 + \sigma^{-2} \sum_{i=1}^{K} P_i\right), \tag{3.4}$$

where σ^2 is the power (variance) of the Gaussian noise $\mathcal{Z}$. It is shown in [14] that formula (3.4) is an upper bound for *sum capacity* of the vector chanel in the case of spreading length $L \geq 1$ (when K components can be distinguished by the receiver). Although it is not in general a tight bound, it remains to express the sum capacity in the case when the power constraints are not "far apart" (precisely when $1/K \sum_{i=1}^{K} P_i \geq L/K \max_{i=1,\ldots,K} P_i$; cf. [18]). Since Formula (3.5)

gives an estimate of the *theoretical maximal bit-rate* that can be achieved by the channel, we see that SINR is indeed crucial within this setting.

Let us now consider emitters of input components to be distributed in the plane, and let us determine all possible locations of a test receiver, such that the channel has a total capacity above some given threshold at this point.

Parameters

- $y, \in \mathbb{R}^2$, potential location of the receiver,
- $\{X_i\}_{i=1}^{\infty}$ pattern of points in $\mathbb{R}^2$ giving the locations of emitters,
- P_i power emitted from the ith source,
- κ interference factor (due to e.g. spreading, processing gain, degrees of freedom, etc. – see [18]),
- $l(x, y)$ path loss from x to y,
- σ^2 Gaussian noise power,
- $\mathcal{C}_{i_1,\dots,i_K}(y)$ total capacity (obtained from (3.4), assuming that interference from external signals can be considered as additive white Gaussian noise that is commonly used postulate) of the channel jointly operated by emitters located at points $X_{i_1}, \dots, X_{i_K}$, interfering with the signals of all other sources located at the points of Φ whenever the receiver is located at y

$$\mathcal{C}_{i_1,\dots,i_K}(y) = \frac{1}{2} \log \left(1 + \frac{\sum_{j=1}^{K} P_{i_j} l(y, X_{i_j})}{\kappa \sum_{i \neq i_k} P_i l(y, X_i) + \sigma^2} \right) . \tag{3.5}$$

- t a threshold on $\mathcal{C}$ ensuring required bit rate.

Now the t-level-set of the capacity $\mathcal{C}_{i_1,\dots,i_K}$ is defined as

$$C_{i_1,\dots,i_K}(y) = \{ y \in \mathbb{R}^2 : \mathcal{C}_{i_1,\dots,i_K}(y) \geq t \} . \tag{3.6}$$

In practice the bandwidth factor is introduced in (3.5), and the logarithm has to be considered in basis 2 so as to interpret the capacity in bps; but such considerations will not be needed in this section where we will limit ourselves to qualitative considerations on the level sets defined by Equation (3.6).

- **Case** $K = 1$ When $K = 1$, we can recognize in (3.6) Model 3 with $\Phi = \{X_i\}$, $a_i = e^{2t}$, $b_i = e^{2t} - 1$, $c_i = \sigma^2(e^{2t} - 1)$, and $S_i = P_i$.
- **Case** $K = 1$ **with fading** Assume there is a random fading in addition to attenuation, that is for all y and all i, there is a random variable $Z_i(y)$ such that the power received at location y from the ith source is $P_i Z_i(y) l(y, X_i)$ in place of $P_i l(y, X_i)$. Then, we find again Model 3 with the functional extension alluded to in §2.3 with $S_i(y) = Z_i(y) P_i$. Mathematical results on this case are gathered in §A.2.2.

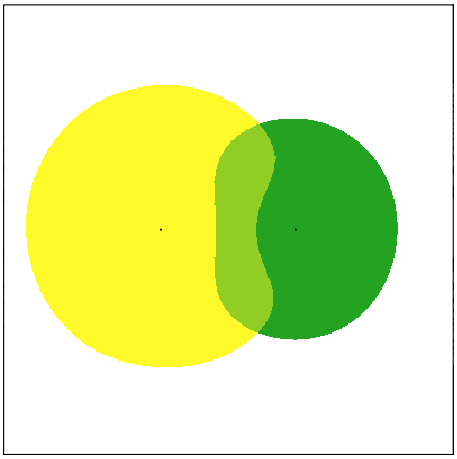

Figure 1: Level sets for $K = 1$

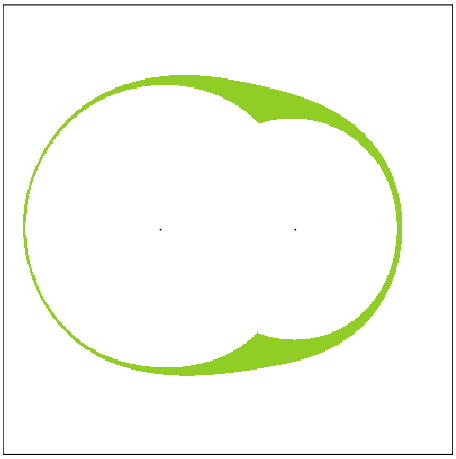

Figure 2: Level sets for $K = 2$

- **Case** $K > 1$ In the case $K > 1$ one has to introduce the point process $\Phi^{(K)}$ of all K-tuples of points of Φ. Within this setting (where the underlying point process lies in $\mathbb{R}^{2K}$ for K-vector channels), one can recognize in (3.6) a set of the form (2.1) with appropriate matrices associated to the points of $\Phi^{(K)}$. The case with fading can be considered along the same lines.

The level sets of the capacity function are exemplified for $K = 1$ and $K = 2$ and for two antennas on Figures 1 and 2. These pictures were obtained using the simulation tool described in §A.4. The colored regions of Figure 2 represent the increase of the level sets (based on the same threshold as in Figure 1) when moving from $K = 1$ to $K = 2$, whereas the white areas in the neighborhood of the antennas correspond to the level sets of the case $K = 1$ (also given in Figure 1 for the very same pattern).

Note that in contrast with what happens in the Boolean model, where there is no interaction between cells, the local configuration has an important impact on the geometry of the level sets of interest here: e.g. as illustrated by Figure 1 in the case $K = 1$, two adjacent antennas fight each other for space, with as a result, shrunken versions of both cells in the area located between the two antennas. So we see that as mentioned in the introduction, irregularities in the antenna patterns result into fluctuations in the geometry of the cells.

Figures 3 and 4 represent the multiple antenna case, which is the main object of the present study. In Figure 3, which bears on the case $K = 1$, there is one randomly chosen color per antenna level set. In Figure 4 (where $K = 2$), there is one randomly chosen color for each pair of antennas that admits a non-empty level set. The convention concerning the white areas in the direct neighborhood of antennas is the same as above). As one can check on this example, the gain of coverage when moving from $K = 1$ to $K = 2$ may be substantial: the uncovered zones (in white on Figure 3) are completely colored on Figure 4. For Figures 3–6 we took as reference [Case 4] of § A.4.2.

In the following sections, we look at more specific examples that stem from practical implementations of the CDMA protocol.

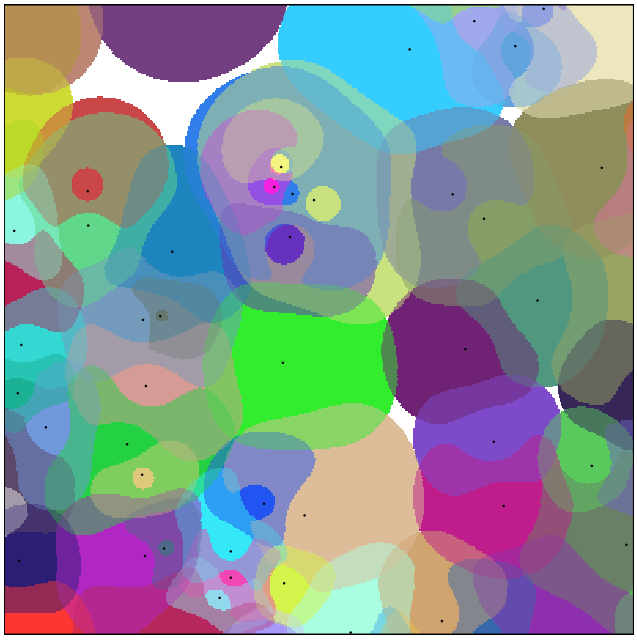

Figure 3: Level sets for $K = 1$

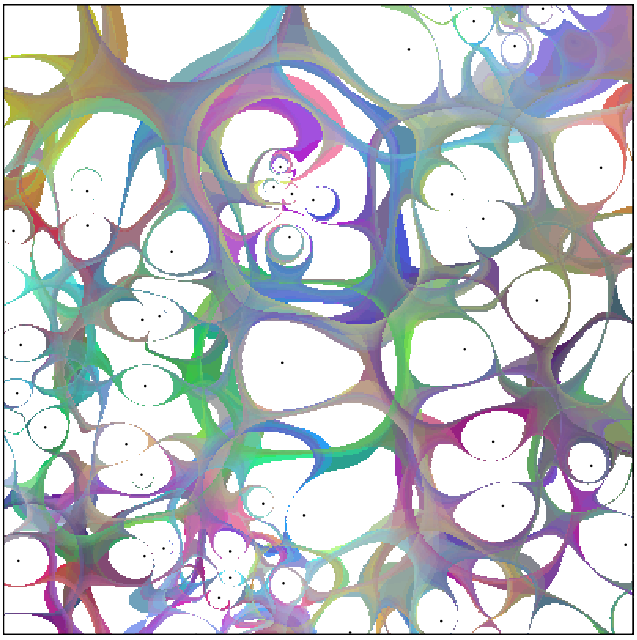

Figure 4: Level sets for $K = 2$

3.2 CDMA Downlink — Handoff Cells

The *downlink* concerns the communications from the *Base Stations* (BS's) to *Mobile Stations* (MS's). We briefly describe how this downlink is established (see e.g. [3]). Some *pilot signal* is emitted by each BS in order to determine the *handoff cells* for each BS. Each BS operates on the same frequency bandwidth and has a set of orthogonal channels (orthogonality is only guaranteed in the absence of multipaths). A MS is *in handoff* of a given BS provided the *pilot signal-to-interference ratio* w.r.t. this BS is larger than an *absolute threshold* We will use the following notation:

- $y, \in \mathbb{R}^2$, potential location of a MS,
- $\{X_i\}_{i=1}^{\infty}$ random pattern point in $\mathbb{R}^2$ (a spatial snapshot) of the locations of BS's,
- P_i total effectively radiated power of the ith BS (these are random variables, that may depend on the number of MS's that are located in the handoff zone of the BS's),
- $l(x, y)$ path loss from $x \in \mathbb{R}^2$ to $y \in \mathbb{R}^2$,
- $Z_i(y)$ shadow fading from the ith BS to point y (random variables),
- N_0 thermal noise power density,
- W frequency bandwidth,
- π_i fraction of the BS power allocated to the pilot signal,
- T_i pilot signal-to-interference absolute threshold;

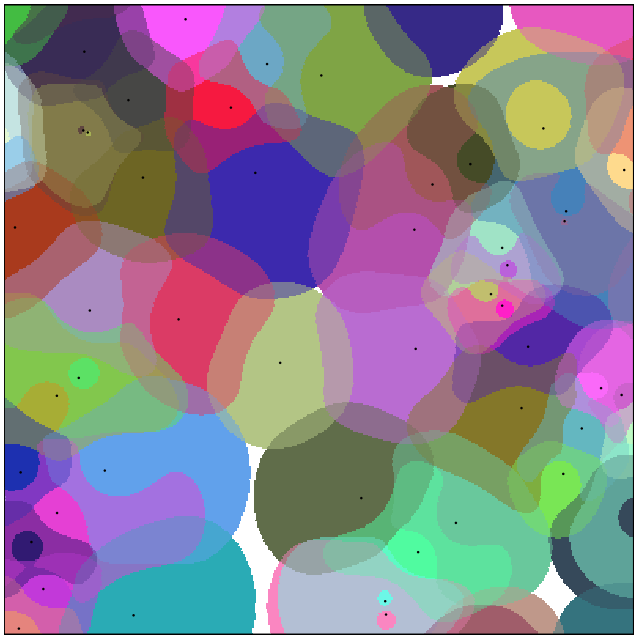

Figure 5: Soft handoff cells without point dependent fading

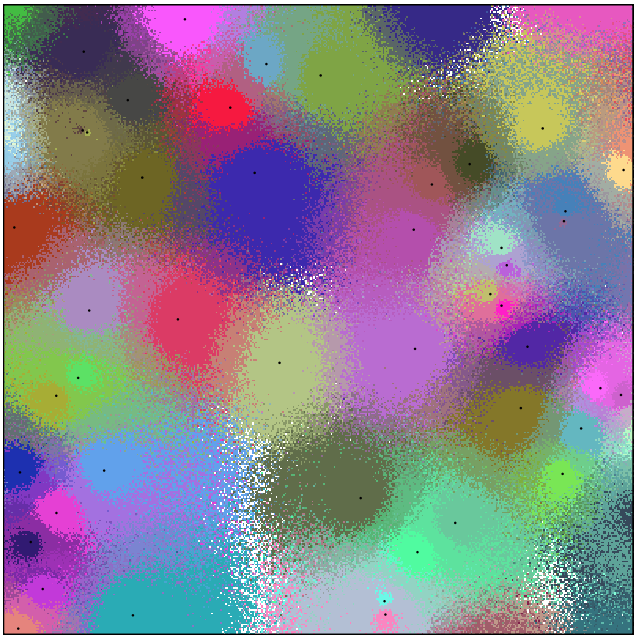

Figure 6: Soft handoff cells with point dependent fading

- $R_i(y)$ pilot signal-to-interference ratio from ith station received at location y, defined as

$$R_i(y) = \frac{\pi_i P_i Z_i(y) l(y, X_i)}{\sum_{j=1}^{\infty} P_k Z_k(y) l(y, X_k) + N_0 W} \,. \tag{3.7}$$

  A simplified model is that where the point dependent shadow fading $Z_i(y)$ is replaced by a random variable Z_i that does not depend on y.

We define the ith station handoff cell $C_i^{(SH)}$ (based on absolute threshold) as the set of possible locations y such that the pilot signal-to-interference ratio $R_i(y)$ received there is above the *absolute threshold* T_i; i.e.,

$$C_i^{(SH)} = \{y : R_i(y) \geq T_i\} \,. \tag{3.8}$$

One can recognize in (3.8) Model 3 with $a_i = \pi_i/T_i$, $b_i = 1$, $c_i = N_0 W$, $S_i(y) = P_i Z_i(y)$, or $S_i = P_i Z_i$ in the simplified case.

The handoff cells of the simplified and the non simplified models are exemplified on Figures 6 and 5, which both bear on the very same point and power pattern. The case with point dependent fading (Figure 6) is that where for all i, an i.i.d. fading $Z_i(y)$ is sampled for each pixel y. Admitting that this assumption is rather far from reality as it does not capture the space correlation of the fading we show Figure 6 as a "worst possible scenario". Real patterns exhibit much more regularity and presumably can be better approximated by the simplified model where the same sample is used for all y (an independent fading variable Z_i is nevertheless sampled for each antenna). As one can check, the simplified cells are essentially a smoothed version of the handoff cells with point dependent fading. In addition, most of the averaged results of the following sections will be identical for both models. It is why we will mainly concentrate on the simplified model in what follows.

By definition, a MS has handoff level H (or is in a H-way handoff) if it belongs to the handoff zone of H different BS's. In this case, there are several situations: in case with hard handoff, one selects one among the H BS's, and power is radiated towards this MS from this BS only. In the soft handoff case, the very same data will be sent by each of these BS's, and this will be used to improve the quality of the downlink communication. Handoff zones of various levels are easy to visualize on the smooth cells of Figure 5.

3.3 Uplink

The *uplink* concerns communications from MS's to BS's. Two key features of the uplink are

- the power control of the signals emitted by the MS's (which is of central importance to reach high capacity);
- interferences between MS's (reverse channels) no matter whether served by the same BS or different BS's.

Each MS uses the same frequency bandwidth (different from that of the downlink) and is recognized by the BS via its permanent and unique code. Each BS participating in the soft-handoff of a given MS assigns to it its own demand for the signal-to-interference ratio at which it wants to receive the signal from this MS. Whether the uplink can be established depends on whether the MS can adapt its power to this demand.

3.3.1 One BS Model

Parameters and typical assumptions (cf. e.g. [17])

- x, location of the BS,
- $\{Y_j\}_{j=1}^k$ random pattern of points in $\mathbb{R}^2$ (a snapshot) of locations of MS's trying to establish uplink communication with the BS,
- M_j the power limit (maximal power) of the jth MS,
- Z_j fading from the jth MS (i.i.d. random variables) to x,
- R information bit-rate,
- ϵ_j^* signal-to-interference ratio demanded for the signal received from the jth MS; this is also the product of the bit-energy-to-interference ratio (defined as the ratio of the received power to the total received power) and of the processing gain W/R. As established in [17], ϵ_j is a set of i.i.d. random variables; randomness here is due to imperfections in power control; measurements show that a typical situation is that where ϵ_j is lognormal.
- ν_j voice activity factor of the jth MS,
- S_j^*: solution of the *power control problem*, that is of the linear system

$$\epsilon_j^* = \frac{W}{R} \frac{S_j^*}{\sum_{l=1,\dots,k,\ l\neq j} \nu_l S_l^* + N_0 W}, \quad j = 1, \dots, k. \tag{3.9}$$

This linear system with unknowns S_j^*, $j = 1, \ldots, k$ admits a solution iff

$$\sum_{i=1,\ldots,k} \frac{R\epsilon_i^* \nu_i}{W + R\epsilon_i^* \nu_i} < 1. \tag{3.10}$$

Whenever a solution exists, the random variables S_j^*, $j = 1, \ldots, k$ are approximately i.i.d. with lognormal distribution (the parameters of this distribution depend on those of the distribution of ϵ_j^* and of k, see [17]). More precisely, the sequence of pairs $\{(\epsilon_j^*, S_j^*)\}$ is i.i.d. and each such pair has a known joint distribution with lognomal marginals.

If there is a solution to the power control problem, then all k MS's could communicate with the BS if they had no limitation in power. Since power is limited, then only those MS's such that

$$M_j l(x, Y_j) Z_j > S_j^* \tag{3.11}$$

can actually meet the minimal power requirement. Assume $M_j = M$ for all j; in view of the fact that the powers S_j^* are i.i.d. and the fadings Z_j are i.i.d. it follows from (3.11) that the probability that a MS located in y meets the minimal power requirement is

$$\mathrm{P}(M.Zl(x, y) > S^*),$$

where S^* and Z are random variables distributed like the S_j^*'s and the Z_j's respectively. So, the probability for this MS to be part of the uplink is equivalent to the probability that point y belongs to the cell centered in x for the Boolean model with parameters $a_0 = M.Z$ and $b_0 = S^*$. In other words, a smoothed version of the uplink cells boil down to a Boolean model (here with only one point). For a survey on mathematical results on the Boolean model, see §A.2.1.

3.3.2 Uplink — Several BS Model

No interference case Consider now the case with several BS's, and denote X_i their locations. For each of them, let Y_j^i, $j = 1, \ldots, k(i)$, denote the locations of a finite number of MS's that could have a feasible uplink to the ith BS in case we could neglect interferences between the uplinks of MS's connected to different BS's. More generally, we will add a superscipt i to indicate that the considered variable is that pertaining to the ith BS. In this no-interference case, the MS's that are part of the uplink of the ith BS are those located in the Boolean model defined by the conditions

$$M_j^i l(Y_j^i, X_i) Z_j^i \geq S_j^{i^*}. \tag{3.12}$$

Case with interference Let us compute the power $I_i(X_i)$ of the interference signals at point X_i, due to MS's that are part of the uplinks of all BS's, except the ith. Since the emission power of MS Y_j^i is $S_j^{i^*}/l(Y_j^i, X_i)Z_j^i$, then

$$I_i(X_i) = \sum_{l \neq i} \sum_{j=1,\ldots,k(l)} \frac{\nu_j S_j^{l^*}}{l(Y_j^l, X_l) Z_j^l} l(Y_j^l, X_i) Z_j^{i,l},$$

where it makes sense to consider that the random variables Z_j^i are i.i.d. and independent of the r.v.'s $S_j^{i^*}$ (see [17]), and similarly that the r.v.'s $Z_j^{i,l}$, which represent the shadow fading from Y_j^l to X_i are i.i.d. and independent of all others.

So, the global uplink is now feasible when taking interference into account whenever

- the systems

$$\epsilon_j^{i^*} = \frac{W}{R} \frac{\widetilde{S}_j^{i^*}}{\sum_{l=1,\dots,k(i),\ l\neq j} \widetilde{S}_l^{i^*} + N_0 W + I_i(X_i)}, \tag{3.13}$$

  $j = 1, \dots, k(i)$, have solutions. But this is guaranteed if the initial uplinks had solutions when ignoring interference in view of the shape of Condition (3.10);

- the power constraint inequalities

$$M_j^i l(Y_j^i, X_i) Z_j^i \geq \widetilde{S}_j^{i^*}, \quad j = 1, \quad k(i), \tag{3.14}$$

  where $\widetilde{S}_j^{i^*}$ is the solution of (3.13), are satisfied for all $j = 1, \dots, k(i)$ and all i. Note that this leads to yet another Boolean model w.r.t. $\{X_i\}$. Of course, there is no guarantee that this holds true if it was holding true in the case without interference.

3.4 Up and Down Link

On can combine the last two models: Model 3 (describing the handoff zones) and a Boolean model for the uplink. An interesting question consists in checking whether the corresponding cells are of the same magnitude. Simulations of the corresponding cells are provided in §5.2.

Note that we do not model any power control in the downlink. In fact for the downlink we focus primarily on the mechanism of handoff zones recognition, in which typically no power control in implemented (pilot signal is not adjusted to a mobile request). In the downlink data channel of a given BS all signals propagate through the same channel and thus are received by a mobile station with equal power. Therefore no power control is required to eliminate near-far problem. The power control is required only at the cell edge to minimize the interference from other cells, which does not however vary very abruptly (e.g. in IS-95 CDMA the dynamic range for the downlink power control is ± 6 dM in contrast to ± 24 dB for the uplink; cf. [11]). This mechanism has presumably small impact on shape of the cells.

4 Performance Characteristics

We summarize here a few basic questions that can be addressed using the generic model described above.

- Coverage by a given cell: what is the probability that a MS located at given point y of space be part of the uplink and or the downlink w.r.t. the ith BS?

- Area of a given cell: what is the distribution of the area of the uplink and or the downlink w.r.t. the ith BS?

- Handoff level of a given point: what is the distribution of the number of antennas H that contain a MS located in y in their handoff zone? Such planar averages receive a natural QoS interpretation. For instance, $1 - \Pr(H = 0)$ represents the frequency with which a mobile station wishing to start a communication at random (in space and time) is able is establish the downlink with at least one BS.

- Contact distribution: for a point y which is covered by exactly k cells, what is the probability that a disc of radius r (resp. a segment of length l and orientation θ) be completely included in the region covered by exactly these k cells? The interest of this characteristic becomes clear when one thinks of this segment as that describing the motion of a mobile during some time interval. The contact distribution then gives the probability that the soft-handoff level remain of level l during this time interval.

5 Some Examples of Results

This section focuses on a few typical examples of applications of the general methodology described in the preceding sections. All results rely on either the explicit/approximation formulas gathered in the appendix, or on the simulation methodology described in §A.4. We both show that the key performance characteristics can be computed from the model parameters, and we show how to use this in order to obtain qualitative and quantitative results on the coverage.

Throughout this section (and the appendix), Φ is a Poisson point process (Poisson p.p. for simplicity) and $\{Z_i\}$ is an independent sequence of independent identically distributed (i.i.d.) random variables characterized by the distribution of Z_0. We sometimes use Z for a generic random Z_i. The default option is that when the underlying Poisson process is non homogeneous; we will denote $\lambda(\cdot)$ its intensity measure and assume that $\lambda(\cdot)$ is non-atomic (thus Φ has no multiple points). In the homogeneous case, we will use λ for the intensity of the point process describing locations of BS's and μ for that of MS's. All numerical examples are based on one of the cases itemized in § A.4.2.

5.1 Shape of Level-Sets of Shannon Capacity

The notation and basic definitions are those of §3.1. We focus on the level sets (3.6), in the case with $K = 1$ (which is directly related to the downlink cell problem) and with simplified fading. We now use the simulation methodology described in §A.4 to obtain samples of the level sets of interest for [Case 2] of § A.4.2. Here the parameters are those of what we will refer to later on as the standard configuration for [Case 2]: $\lambda = 0.04\text{BS/km}^2$, $\epsilon = 13$. On Figure 7, we give the level-sets for t is varying from 0.8 to 0.2. Only the boundaries of the cells are depicted for the sake of easier shape interpretation.

5.1.1 Influence of the Interference Coefficient

Figure 8 also bears on the level-sets for [Case 2] of § A.4.2. On Figure 8 we fix $t = 0.4$ and decrease the interference coefficient $\kappa \to 0$. Observe that for certain values of κ, capacity w.r.t. some given antenna falls below the threshold just in the neighborhood certain other antennas: even in the smoothed version considered here (see §3.2), level sets are not convex, and may even have holes! As one can check, level-sets tend to a Boolean model when κ tends to 0. In the limiting case $\kappa = 0$, cells are spherical. So our first qualitative result states that small interference coefficient allow one to approximate level sets for $K = 1$ by cells of a Boolean model. This will be used for expansions in what follows.

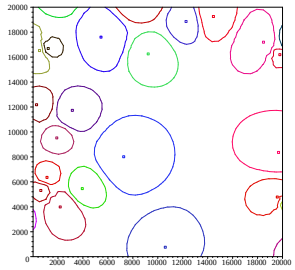
[a] $t = 0.8$

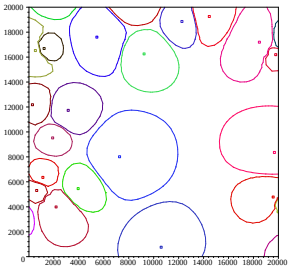
[b] $t = 0.6$

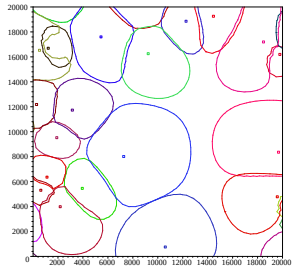
[c] $t = 0.4$

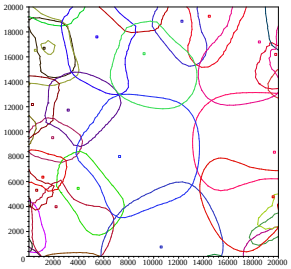
[d] $t = 0.2$

Figure 7: Level-sets of Shannon capacity for the standard configuration.

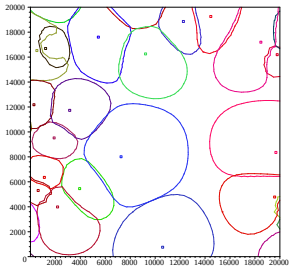
[a] $\kappa = 0.5$

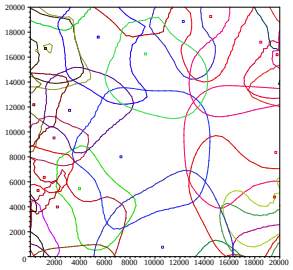
[b] $\kappa = 0.1$

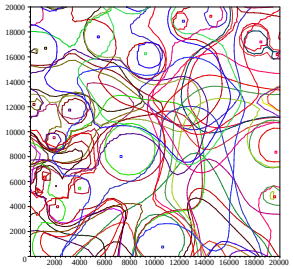
[c] $\kappa = 0.01$

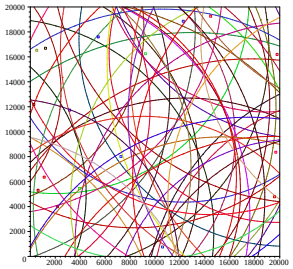
[d] $\kappa = 0$

Figure 8: Level-sets of Shannon capacity at $t = 0.4$. for the standard configuration but with $\kappa \to 0$.

5.1.2 Influence of the Attenuation Coefficient

On Figure 9, we consider [Case 2], but we take a much higher attenuation coefficient, $\alpha = 9$, which may be observed in certain dense urban environments. In this case, the external noise ($\sigma^2 \approx 1.5 * 10^{14}$) makes cells very small. In order to get an acceptable coverage, on has either to densify the pattern of BS's (this is done on Figure 9 a–b where $\lambda = 64\text{BS/km}^2$ is here 16000 times bigger than in the standard configuration) or to magnify antena powers (this is done on Figure 9 c–d, where $\epsilon = 293$ making power about 10^{28} times bigger than in the standard configuration, which is of course non realistic. On Figure 9 e–f, we see $P_i = \infty$ (which is equivalent to $\sigma^2 = 0$). The level-sets are then similar to Voronoi tessellation. Our second qualitative finding states that level sets (or equivalently downlink cells) are closer to Voronoi cells whenever attenuation is stronger, e.g. in urban areas.

5.2 Up and Down Links

In the following simulations, which are again based on the methodology described in §A.4, we assume the configuration of [Case 3] of § A.4.2 for the soft-handoff zone model. As for the uplink, let us take for simplicity the one BS model based on Equation (3.11) with $M_j = 2\text{W}$, Z_j lognormal with $\sigma^2 = 8\text{dB}$ and various values of S_j^*. The two models are jointly presented on Figure 10. The discs with dotted boundaries represent the uplink constraint in its Boolean approximation (see the end of §3.3.1), whereas the non dotted lines represent the boundaries of the smooth version of the downlink cells. Depending on the number of MS's in each cell, either the down or the uplink may be the bottleneck. This is well illustrated by the different patterns observed in Figure 10.

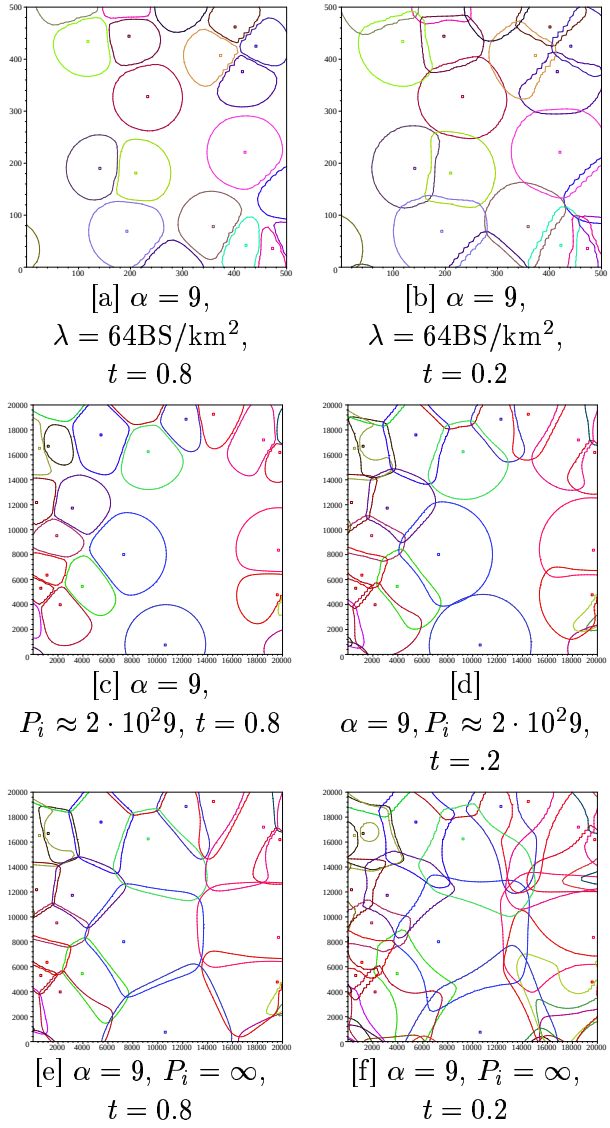

[a] $\alpha = 9$, $\lambda = 64\text{BS/km}^2$, $t = 0.8$

[b] $\alpha = 9$, $\lambda = 64\text{BS/km}^2$, $t = 0.2$

[c] $\alpha = 9$, $P_i \approx 2 \cdot 10^2 9$, $t = 0.8$

[d] $\alpha = 9, P_i \approx 2 \cdot 10^2 9$, $t = .2$

[e] $\alpha = 9$, $P_i = \infty$, $t = 0.8$

[f] $\alpha = 9$, $P_i = \infty$, $t = 0.2$

Figure 9: Level-sets of Shannon capacity for the standard configuration with higher attenuation and more dense proces of BS's, or magnified antenas powers.

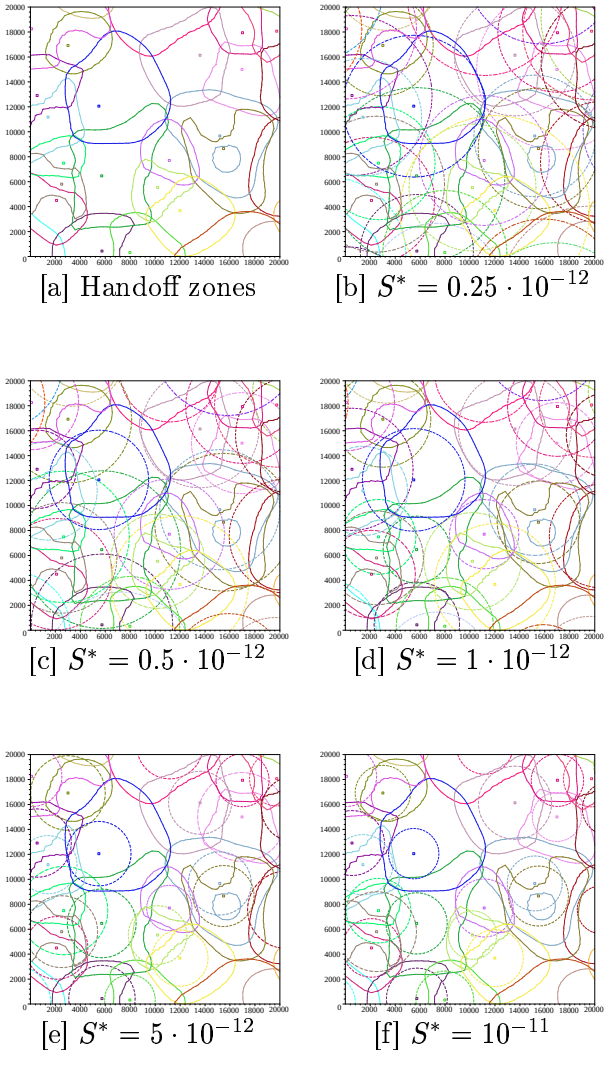

[a] Handoff zones

[b] $S^* = 0.25 \cdot 10^{-12}$

[c] $S^* = 0.5 \cdot 10^{-12}$

[d] $S^* = 1 \cdot 10^{-12}$

[e] $S^* = 5 \cdot 10^{-12}$

[f] $S^* = 10^{-11}$

Figure 10: Up-and-down link model combined. S_i^* varies giving up-link cells on average larger or smaller than handoff zones.

5.3 Network QoS

We again focus on Model 3.

5.3.1 Coverage

The probability $p(r)$ that a typical antenna contains a mobile, located at distance r, in its cell is an important parameter, already discussed in the introduction. Exact values of $p(r)$ can be obtained from the singular integral representation of §A.2.2 or from the expansion technique of §A.3.1. The results of the two methods are plotted on Figure 11. The thick black line represents the result of the singular integral representation (A.10). The blue and red curves /thin upper and lower line/ represent the first, second, 14-th and 15-th order expansion based on the approximation of this probability in the neighborhood of the Boolean limit (see §A.3.1).

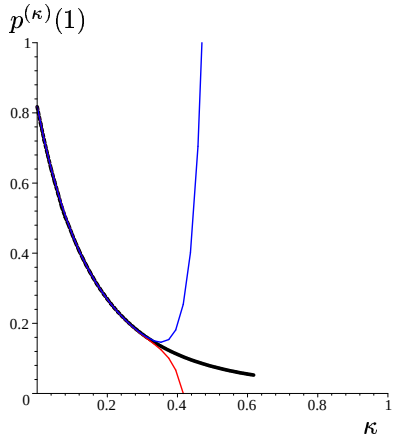

Figure 11: Probability of coverage as a function of the interference coefficient

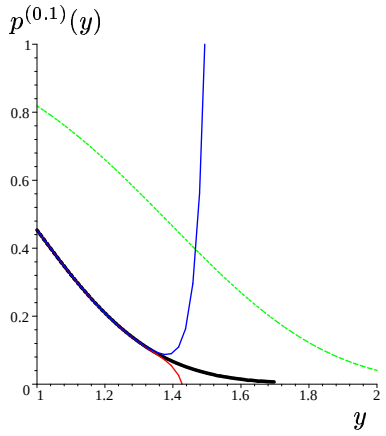

Figure 12: Probability of coverage as a function of the distance.

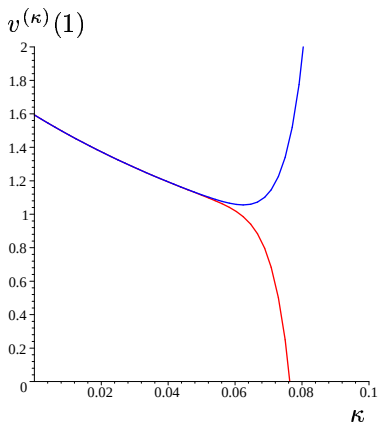

Figure 13: Mean cell area as a function of the interference coefficient

We consider [Case 1] of § A.4.2, with $\lambda = 1$. Figure 11 gives the value of $p(1) = p^{(\kappa)}(1)$ in function of κ. Figure 12 gives the mapping $r \to p(r)$ for $\kappa = 0.1$. The thick black line represents the result of the integral representation (A.10); the blue and red curves /thin upper na lower lines/ represent 14-th and 15-th order expansion based on the perturbation approximation; the light green curve /thin dashed line/ represents the Boolean case ($\kappa = 0$).

5.3.2 Mean Cell Area

The numerical scheme of §A.3.1 for the mean area of the typical cell of Model 3 with data as in [Case 1], $\lambda = 1, m = 1$ is plotted on Figure 13.

5.3.3 Contact Distribution

In this section we consider Model 3. For a point x which is covered by exactly k cells, we denote

- R the largest random variable such the ball $B(x, R)$ is covered by exactly k cells too (namely the largest ball where the reception conditions do not change)
- L the longest segment with extremity x such that the whole segment is covered by exactly k cells.

These questions are related to the so called spherical and linear contact distribution. Analytical answers to this question are only available in the Boolean case (see (A.6) and (A.6) below), and for $k = 0$. Thanks to the stationarity and the isotropy of the model, we can choose $x = O$, without loss of generality. We concentrate on simulation results for Model 3 all based on the conditional simulation algorithm described in §A.4.2. In order to obtain samples with the right condition (namely that the origin is covered exactly k times), it is enough to take $n = p = 1$ and $z_1 = z_1' = 0$ and $n_1 = n_1' = k$ in this algorithm. In the following simulations, we take as reference [Case 4] of § A.4.2. All figures bear on an observation window $[-5\text{km}, 5\text{km}]^2$ and are based on a circular influence window with radius $R' = 40\text{km}$.

Figure 14 focuses on conditional samples allowing one to estimate the fluctuations of L and R.

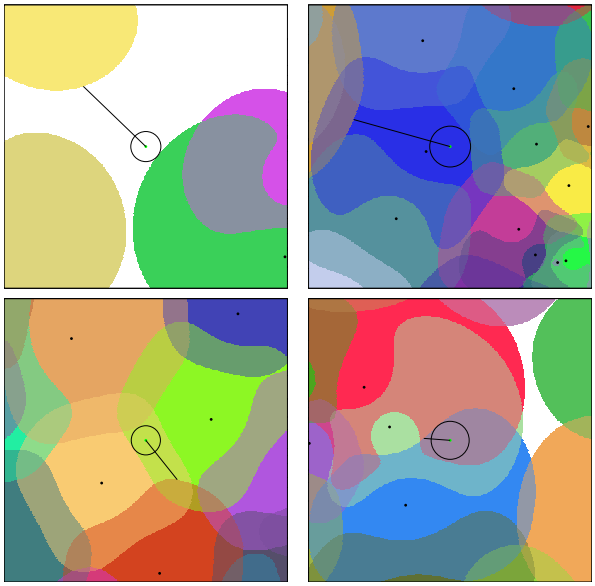

Figure 14: Conditional sample of Model 3. Point O is covered 0,1,2 or 3 times. The corresponding samples of L and R are also given.

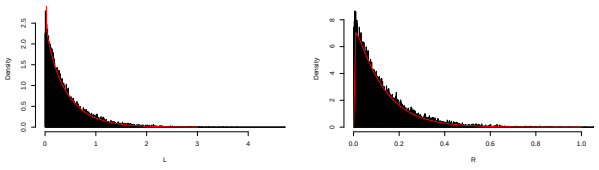

Figure 15: Histogram of L (on the right) and R (left) given O is covered 0 times.

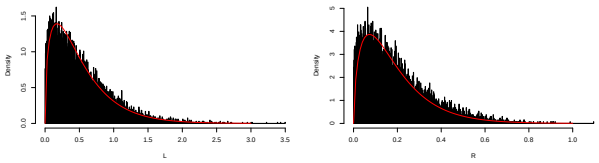

Figure 16: Histogram of L (on the right) and R (left) given O is covered 1 times.

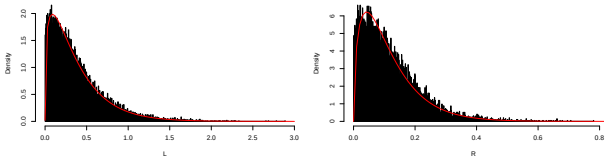

Figure 17: Histogram of L (on the right) and R (left) given O is covered 2 times.

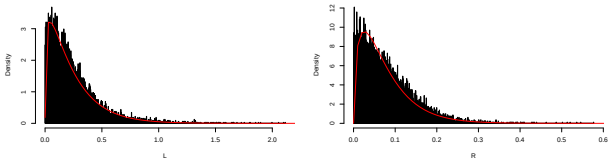

Figure 18: Histogram of L (on the right) and R (left) given O is covered 3 times.

handoff level	EL	$varL$	ER	$varR$
0	0.423 km	0.191 km^2	0.121 km	0.013 km^2
1	0.521 km	0.182 km^2	0.186 km	0.021 km^2
2	0.375 km	0.107 km^2	0.116 km	0.008 km^2
3	0.239 km	0.047 km^2	0.075 km	0.003 km^2

Figure 19: Mean and variance.

Figures 15, 16 17 and 18 give the histograms of the random variables L and R as obtained from the simulator. Table 19 gives more global results such as the mean of L and R. For instance, for this set of values, if there is no reception at a given location, one must move away 400 meters away in mean to recover good reception again.

The numbers of samples on which these histograms are based are 24000 for $k = 0$, 13000 for $k = 1$, 19000 for $k = 2$ and 15000 for $k = 3$. We limited ourselves to testing the hypothesis of Gamma distributions. The Kolmogorov-Smirnov test was applied using the R package. The hypothesis was accepted for the linear case when $k = 0$, and rejected in all other cases.

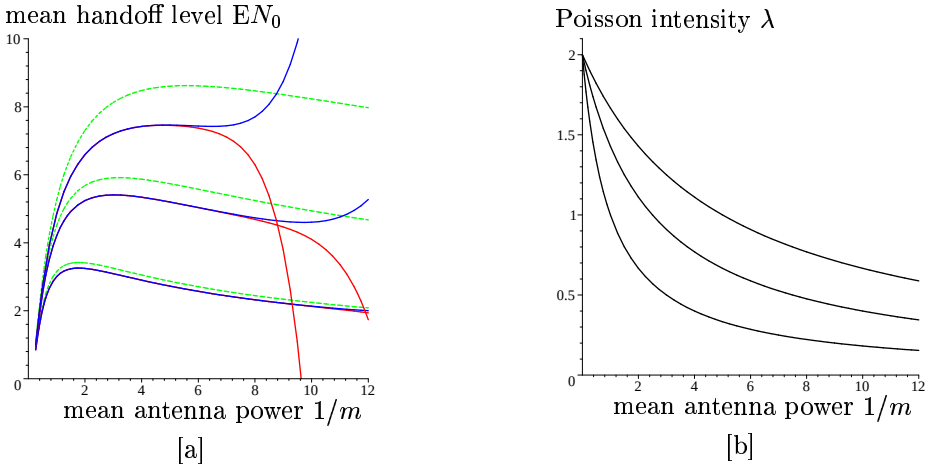

Figure 20: [a] Mean handoff as a function of mean antenna power $1/m$ under budget constraint (5.15) with $C = 1000, C_\lambda = 500$ and from the top: $C_m = 1, 2, 5$. [b] Solutions of (5.15) as functions $\lambda = \lambda(1/m)$ for the same set of parameters; curves form top to bottom.

Notice that for all quantities pertaining to spatial joint distributions (such as the probability that all points of a given segment or of a given ball have soft handoff level with a prescribed value), the difference between simplified fading and point dependent fading actually matters. In that, the distributions which are studied in this section are only approximations of the quantities of practical interest for mobile communications, since the distributions in question bear on the smoothed versions of the cells only.

5.4 Parametric Optimization

We now show to solve a typical optimization problem using our analytical tools. The problem is that of the tradeoff between densification and increase of station power.

Suppose an operator has a total budger of C per km^2, and that the cost of one antenna is C_λ, whereas increasing the power of one antenna by 1W costs C_m. In order to use the total budget in the most efficient way, the operator may wish to maximize one of the average local characteristics such as the expected mean handoff level for a typical location (EN_0), under the above cost constraint.

Let us now show how to translate the last example into a simple problem within our setting. The cost constraint translates into the condition

$$\lambda C_\lambda + C_m \lambda / m = C. \tag{5.15}$$

We solve this equation in $\lambda = \lambda(m)$ and use (A.13) together with the perturbation formula for the mean area v_0 (see the end of §A.3.1) to plot EN_0 as a function of m. Figure 20 a shows such plots, for $C = 10, C_\lambda = 5$ and three choices of $C_m = 1, 2, 5$ (curves from top to bottom). The case considered here is that of the Shannon capacity level-sets as in [Case 1] of § A.4.2 with $\kappa = 0.01$, $t = 0.35$ (this is the same model as that considered in §5.3.1). Blue curves /thin uper line in each set/ represent 14 th order polynomial approximations and read ones /thin lower lines/ approximations of order 15. So our approximation is fine until these two colors split, for each case of C_m. (The light green curves /thin dashed lines/ represent the limiting Boolean model with $\kappa = 0$.) Part b of Figure 20 shows the corresponding functions $\lambda = \lambda(1/m)$. For

instance, for $C_m = 2$, the optimal configuration has $\lambda^* \sim 0.9$ antennas per square unit and each antenna has a power $1/m^*$ of approximatively 3 W. The same type of optimization could be applied to other local characteristics such as the probability that a typical point be covered. For this, on should use the expression for volume fraction of Model 3 (see (A.16) and (A.12) in §A.2.2).

6 Conclusions, Future Work

We have proposed a generic stochastic model allowing one to estimate spatial averages of key geometrical characteristics of large CDMA based wireless networks taking into account the irregular nature of point patterns.

The model allows one to address both high level representations, such as level sets of Shannon's capacity function, and specific issues pertaining to the down and the uplink.

In the Poisson case, the model leads to several analytical results allowing for the prediction of QoS and the optimization of the architecture. Adapted simulation schemes offer another natural way of estimating geometrical characteristics which cannot be described in an analytical way.

The framework of stochastic geometry already offers a significant number of mathematical results that should allow one to approach further problems within this setting. We conclude the paper with a list of problems which it should be possible to address using these tools.

6.1 Refined Cell Models

Here are a few natural extensions of our basic model.

6.1.1 External Noise as a Random Field

Thermal noise was represented as a random variable and not as a random field. We can easily represent this noise as a shot noise created by yet another pattern of sources (modeled by another point process Φ') of powers S'_i with a possibly different attenuation function l'. In both downlink and uplink models this would corresponds to introducing another term depending on the location $I_{\Phi'}(y)$ (or $I_{\Phi'}(x)$ respectively) in the denominator of e.g. Eq. (3.7), where

$$I_{\Phi'}(z) = \sum_{X'_i \in \Phi'} S'_i l'(z - X'_i)\,.$$

It is easy to check that is is yet another incarnation of the generic model.

6.1.2 Directional Antennas

Up to now we have considered attenuation function of the form $\mathrm{const}\big(\max(r_0, |x|)\big)^{-\alpha}$), which corresponds to the case of isotropic antennas with ideal Hertzian propagation. When emitter antennas are directional, a mark $\tau_i \in \mathbb{R}^2$ should be used for describing the direction vector of antenna i. The effect of antenna i located at z_i on point y can then be modeled e.g. by the following type of attenuation function

$$L(\tau_i, y - z_i) = l(y, z_i)((\tau_i) \cdot (y - z_i))/|y - z_i|$$

where $z_1 \cdot z_2$ is the scalar product of vectors z_1, z_2.

6.1.3 Relative Threshold

In the definition of the downlink, in the soft-handoff case, besides the absolute threshold condition given by (3.8), there is often a *relative threshold* condition, which consists in accepting the ith station to participate in the handoff of the MS located at y only if

$$R_i(y) \geq \theta \max_{j/R_j(y)\geq T_j} R_j(y), \tag{6.16}$$

where $\theta < 1$ is some threshold and where $R_i(y)$ is the ratio defined in (3.7). The rationale for this is that power should only be radiated by the ith BS towards a given MS provided the signal received by the MS from this BS is not marginal compared to the best. Note that this boils down to the following condition: the ith BS participates in the handoff of the MS located in y if in addition to (3.8)

$$\pi_i P_i Z_i(y) l(y, X_i) \geq \theta \max_{k/R_k(y)\geq T_k} \pi_k P_k Z_k(y) l(y, X_k)\,. \tag{6.17}$$

The geometry of (6.17) is a special case of the (generalized) generic model too, with $N_i = card(\Phi)$; all entries of $A_i(y)$ and $B_i(y)$ are zero but for $(A_i)_{ji}(y) = \pi_i P_i Z_i(y)$, $j \neq i$, and $(A_i)_{jj}(y) = -\theta\pi_j P_j Z_j(y) 1_{R_j(y)\geq T_j}$, $j \neq i$, $j \in \mathbb{N}$.

The geometry of the combination of (3.8) and (6.17) is also a special case of the generic model with $N_i = card(\Phi)$; for instance, in the simplified fading model, all entries of A_i and B_i are zero but for $(A_i)_{ji} = \pi_i P_i Z_i$, $j \neq i$, $(A_i)_{jj} = -\theta\pi_j P_j Z_j$, $j \in \mathbb{N}$, $j \neq i$, $(A_i)_{ij} = -P_i Z_i$, $j \neq i$, $(A_i)_{ii} = (\frac{\pi_i}{T_i} - 1) P_i Z_i$, and $(B_i)_i = N_0 W$.

6.2 Capacity

The capacity problem should be understood in the following sense: assume given an infinite population of MS's located at points $\{Y_j\}$, $j \in J$, and a set of antennas $\{X_i\}$, $i \in I$. We will call *allocation* a function that associates to J a subset J', and to each index $j \in J'$ a single index $a(j) \in I$. Such an allocation defines the subset $\{Y_l^i\}$, $l = 1, \ldots, k(i)$ of the set of points $\{Y_j\}$ of locations of MS's with a link to the ith BS (we consider here the case of hard handoff).

Assume that the total power radiated by the ith BS depends on the number of stations that are in its handoff zone. Then an increase in the population of MS's leads to a higher power emitted, and possibly to a shrunken handoff zone. This results into a natural *downlink capacity problem*. An allocation a defines the total power that the ith BS should radiate, which one could for instance take proportional to the cardinal of the set $\{Y_l^i\}_l$. We will then say that

- this allocation is *feasible* w.r.t. the downlink (resp. the uplink) if it is such that for all l, the point $\{Y_l^i\}$ is located in the handoff cell of the ith BS (resp. the point $\{Y_l^i\}_l$ satisfies the power constraints inequality (3.14) w.r.t. the ith BS);
- this allocation is *maximal* w.r.t. the downlink (resp. the uplink) if for all i, there exists a $j \notin J'$ such that when adding the jth MS to the handoff zone of one of the BS's, then the new allocation is not feasible w.r.t. the downlink (resp. the uplink).

6.3 Mobility

Mobility was only addressed here through the empirical evaluation of the linear contact distribution, which receives a natural interpretation in terms of the time a mobile keeps emis-

sion/reception conditions that remain the same. There is a large set of open questions along these lines. Let us quote two of them:

- What is the nature of the stochastic process describing the evolution of the quality of emission/reception or that of the handoff level, for a mobile moving along a random line of the plane?
- For a given mobility pattern, there is a coupling between the positions of the MS's, the resulting power control, and the geometry of cells. This so called *cell breathing* is a fascinating time-space phenomenon too, which might be approached via these tools when adding some time evolution mechanisms for cells.

6.4 Refined Probabilistic Models

As for parametric models, Poisson point processes might be too rough an approximation for representing the fluctuations of the location of antennas. Poisson Gibbs fields, with e.g. a repulsive potential might offer a more versatile model.

Appendix A: Summary of Mathematical Results

In this section we make a survey of mathematical formulas and simulation schemes which allow one to compute or to approximate quantities of interest related to our generic model. We will concentrate mainly on special case 1 (the Boolean Model) and case 3 (Model 3) of section 2.

A.1 Typical Cell

The *typical cell* $C(x;\Phi\cup\{(x,Z)\})$ attached to a point located at x is by definition the cell of point x for the pattern $\Phi\cup\{(x,Z)\}$, where Φ is the Poisson p.p. and $Z=(A,B)$ is an "additional mark" distributed like the other marks and independent of Φ. If the Poisson point process is homogeneous, the characteristics are the same for all points x and we will speak of the typical cell.

A.2 Exact Formulas

A.2.1 Boolean Model

The notation is that of §2. The formulas of this section are classical ones (see e.g. [15], chapter 3, pp. 59–96).

Coverage by a typical cell : Denote by $p_x(K)=\Pr(K\subset C(x;\Phi\cup\{(x,Z)\})$ the probability that a test compact set $K\subset\mathbb{R}^2$ is covered by the typical cell located at x. We have

$$p_x(K)=F_{c_0/a_0}(\underline{l}(K-x))\,, \tag{A.1}$$

where F_{c_0/a_0} is the d.f. of a_0/c_0 and $\underline{l}(A)=\inf_{y\in A}l(y)$, $K-x=\{y-x:y\in K\}$. In particular for a single point $K=\{y\}$, $p_x(y)=F_{c_0/a_0}(l(y-x))$. The probability that the test set K is intersected by the typical cell is $F_{c_0/a_0}(\overline{l}(K-x))$ where $\overline{l}(A)=\sup_{y\in A}l(y)$.

Mean area of the typical cell :

$$v_x = \mathrm{E}\Big[\Big|C(x;\Phi\cup\{(x,Z)\})\Big|\Big]. \tag{A.2}$$

It can be then obtained from the $p_x(\cdot)$ function by the relation

$$v_x = \int_{\mathbb{R}^2} p_x(y)\,dy. \tag{A.3}$$

Number of cells : covering (resp. intersecting) a test compact set K is Poisson distributed with parameter

$$\begin{aligned} \underline{\lambda}(K) &= \int_{\mathbb{R}^2} F_{c_0/a_0}(\underline{l}(K-x))\,\lambda(dx), \\ (\text{resp. } \overline{\lambda}(K) &= \int_{\mathbb{R}^2} F_{c_0/a_0}(\overline{l}(K-x))\,\lambda(dx)). \end{aligned}$$

In particular the *capacity functional* of $\Xi=\bigcup_i C_i$ of the test compact set $K\subset\mathbb{R}^2$, which is defined by $T_\Xi(K)=\Pr(\Xi\cap K\neq\emptyset)$, is given by the formula

$$T_\Xi(K) = 1-\exp\Big[-\overline{\lambda}(K)\Big]. \tag{A.4}$$

Volume fraction of the coverage process : $p = \mathrm{P}(0\in\Xi)$ is a characteristic of a stationary coverage process

$$p = T_\Xi(\{0\}) = 1-\exp\left(\lambda\int_{\mathbb{R}^2} F_{c_0/a_0}(l(-x))\,\lambda(dx)\right). \tag{A.5}$$

Linear contact distribution function of Ξ : is the conditional distribution function of the distance from a test point y in a test direction z to Ξ, given $x\notin\xi$

$$\begin{aligned} H_{[y,z]}(r) &= \Pr([y,y+rz]\cap\Xi\neq\emptyset | y\notin\Xi) \\ &= 1-\frac{e^{-\overline{\lambda}([y,y+rz])}}{e^{-\overline{\lambda}(y)}}, \end{aligned} \tag{A.6}$$

$r\geq 0$. Similarly the *spherical contact distribution function* is

$$\begin{aligned} H_{B(y,1)}(r) &= \Pr(B(x,r)\cap\Xi\neq\emptyset | y\notin\Xi) \\ &= 1-\frac{e^{-\overline{\lambda}(B(y,r))}}{e^{-\overline{\lambda}(y)}}, \end{aligned} \tag{A.7}$$

$r\geq 0$, where $B(x,r)$ is the ball centered at 0 and with radius r. One can consider also these contact distribution functions of a typical cell located at y. Then $\exp(\overline{\lambda}(\cdot))$ has to be replaced in the above formulas by $1-F_{c_0/a_0}(\overline{l}(\cdot-x))$.

A.2.2 Model 3

Coverage by a typical cell located at x: for one-point test set $K = \{y\}$, assuming that $b > 0$ a.s.

$$p_x(y) = \mathrm{P}\Big((\frac{a}{b} - 1)Sl(y-x) - \frac{c}{b} - I_\Phi(y) \geq 0\Big) \tag{A.8}$$

The shot-noise term I_Φ is independent of other terms and its distribution can be known via its transforms. For example the *Fourier transform* of the vector $(I_\Phi(y_1, \ldots, y_n)$ is given by

$$\begin{aligned}\psi_I(\xi_1, \ldots, \xi_n, y_1, \ldots, y_n) &= \mathrm{E}\exp\Big[-i\sum_{i=1}^{n}\xi_i I_\Phi(y_i)\Big] \\ &= \exp\Big[\int_{\mathbb{R}^2}\Big(\varphi_S\Big(\sum_{i=1}^{n}\xi_i l(y_i - x)\Big) - 1\Big)\,\lambda(dx)\end{aligned} \tag{A.9}$$

where ψ_S is the Fourier transform of S. Knowing the Fourier transform $\psi_I(\xi, y)$ of $I_\Phi(y)$ one can reduce calculation of $p_x(y)$ to the singular contour integral (to be understood in the principal value sense):

$$p_x(y) = \frac{1}{2} - \frac{1}{2i\pi}\int_{\mathbb{R}}\frac{\rho(\xi, x, y)}{\xi}\,d\xi, \tag{A.10}$$

where

$$\rho(\xi, x, y) = \psi_I(-\xi, y)\mathrm{E}\exp\Big[-i\xi\frac{1}{b}((a-b)Sl(y-x) - c)\Big]$$

(see [1] for details and the proof). Coverage, and intersection with a more general test set K, and in particular contact distribution functions have to be studied via simulation.

Mean area of the typical cell : it can be obtained from Formula (A.3) with $p_x(y)$ for Model 3.

Number of cells covering a test point y (denoted N_y): this can be analyzed in terms of its factorial moments $\mathrm{E}[N_y^{(n)}]$, where $N^n = N(N-1)\ldots(N-n+1)^+$, $(t^+ = \max(t, 0))$, which can be expressed as follows

$$\begin{aligned}\mathrm{E}[N_y^{(n)}] \;=\; &\int_{\mathbb{R}^{2n}}\mathrm{P}\big(y \in \bigcap_{k=1}^{n} C\Big(x_k; \Phi\bigcup_{i=1}^{n}\{(x_i, Z_i)\}\Big)\big) \\ &\lambda(dx_1)\ldots\lambda(dx_n)\,,\end{aligned} \tag{A.11}$$

where Φ is the original marked Poisson p.p. and $\{Z_i\}_{i=1}^n$ is an independent sequence of mutually independent vectors distributed as the generic mark; this relation holds provided the integral on the right hand side is finite. If Φ is a homogeneous Poisson p.p. with intensity $\lambda(dx) = \lambda dx$ then for each $x \in \mathbb{R}^d$

$$\begin{aligned}&\mathrm{E}[N_y^{(n)}] = \mathrm{E}[N_0^{(n)}] \\ =\; &\lambda^n\int_{(\mathbb{R}^d)^n}\mathrm{P}\Big(0 \in \bigcap_{k=1}^{n} C\Big(x_k; \Phi\cup\bigcup_{i=1}^{n}\{(x_i, Z)\}\Big)\Big) \\ &dx_1\ldots dx_n,\end{aligned} \tag{A.12}$$

provided the integral is finite. In particular, for $n = 1$

$$\mathrm{E}[N_0] = \lambda v_0, \tag{A.13}$$

where v_0 is the area of the typical cell. The distribution of N_x can be derived using the formula

$$\mathrm{P}(N_x = n) = \frac{1}{n!} \sum_{k=0}^{\infty} (-1)^k \frac{\mathrm{E}[N_x^{(n+k)}]}{k!}, \tag{A.14}$$

which follows from the well-known expansion of the generating function.

In certain cases, there is a deterministic upper bound on N_x, which allows one to reduce the characterization of its law via (A.14) to a finite number of integrals of the type (A.12): for $a_i, c_i > 0$ the following inequality

$$\sum_{k=1}^{n} \frac{b_{i_k}}{a_{i_k}} < 1 \tag{A.15}$$

is a necessary condition for the set of cells C_{i_k}, $k = 1, \ldots, n$, to have a common nonempty intersection. So Condition (A.15) gives bounds on the number N_y of cells covering y: suppose that the distribution of the mark $A_0 = (a_0, b_0, c_0)$ is such that b_0/a_0 is bounded away from 0; i.e., $b_0/a_0 \geq \rho$ a.s. for some constant $\rho > 0$; then for any y, $N_y < 1/\rho$ almost surely.

Volume fraction of the coverage process : using factorial moments of N_x we can write

$$\mathrm{P}(x \in \Xi) = \sum_{k=1}^{\infty} \frac{(-1)^{k+1}}{k!} \mathrm{E}[(N_x)^{(k)}]\,. \tag{A.16}$$

Further characteristics : The number of cell covering (intersecting) more general test set, as well as the contact distribution function of the whole process, have to be studied via simulation.

A.3 Perturbation Formulas

Under the term perturbation analysis we understand various results describing the behavior of the model under some (typically small) changes of parameters. These results are in terms of limits, (partial) derivatives, higher derivatives, expansions of model characteristics with respect to some model parameters. They can can be used either for planing issues (e.g. marginal cost), or for numerical approximations of the model characteristics.

A.3.1 Approximation of Model 3 via Perturbation of a Boolean Model

We briefly review here the results from [1] concerning convergence of the generic model to the Boolean model. Note that the cells of Ξ given by (2.1) are not mutually independent because of the presence of the shot-noise variable I_Φ. However, if we assume $b = 0$ a.s. the cells are independent, and Ξ is a Boolean model. One can then consider the following perturbation of this Boolean model: assume that $b \to 0$ in some sense. It is shown [1] that under some natural

technical conditions, typical cells and their characteristic as capacity functional (in particular coverage probabilities $p_x(y)$), mean volume v_x, number of cells hitting a compact set (so N_x and volume fraction p) etc., all tend is some sense to their counterparts in the Boolean model.

Moreover the first order and higher order corrections that should to be applied to the characteristics of the Boolean model in order to approach the characteristics of the generic model are also known [1]. More specifically, let

$$C^{(\kappa)} = C_x^{(\kappa)} = \left\{ y \in \mathbb{R}^2 : aSl(y-x) \geq \kappa b I_\Phi(y) + c \right\}, \tag{A.17}$$

$I_\Phi(y)$ is given by (2.2), x is fixed and (a, b, c, S) is an additional mark independent of Φ, with $c > 0$ almost surely. We will denote by $p_x^{(\kappa)}(y) = \mathrm{P}(y \in C_x^{(\kappa)})$ the point coverage probably and by $v^{(\kappa)} = \mathrm{E}|C_x^{(\kappa)}|$ the mean area of $C_x^{(\kappa)}$.

Assume that $b > 0$ a.s. (to avoid conditional distributions) and let $F_*(u) = F_*(u; y)$ denote the distribution function of the random variable $(aSl(y) - c)/b$; i.e.,

$$F_*(u) = F_*(u; y) = \mathrm{P}\left(\frac{aSl(y-x) - c}{b} \leq u \right). \tag{A.18}$$

Let F_* admit the following Taylor approximation at 0

$$F_*(u) = F_*(0) + \sum_{k=1}^{h} \frac{F_*^{(k)}(0)}{k!} u^k + \mathcal{R}_*(u) \tag{A.19}$$

and $\mathcal{R}_*(u) = o(u^h) \quad u \searrow 0$, where $F_*^{(k)}(0) = F_*^{(k)}(0; y)$ are the derivatives of $F_*(u; y)$ w.r.t. u at $u = 0$.

- If (A.19) holds for some $h \geq 1$ then

$$\begin{aligned} p_x^{(\kappa)}(y) &= \mathrm{P}\Big(aSl(y-x) \geq c \Big) \\ &\quad - \sum_{k=1}^{h} \kappa^k \frac{F_*^{(k)}(0)}{k!} \mathrm{E}\big[(I_\Phi(y))^k \big] + o(\kappa^h), \end{aligned}$$

  provided $\mathrm{E}[(I_\Phi(y))^{2h}] < \infty$.

- If the random field $I_\Phi(y)$ is stationary, (A.19) holds for for some $h \geq 1$ and all $y \in \mathbb{R}^2$, and moreover if the remainder term $\mathcal{R}_*(u) = \mathcal{R}_*(u; y)$ is bounded $|\mathcal{R}_*(u, y)| \leq \mathcal{H}_1(u)\mathcal{H}_2(y)$ where $\mathcal{H}_1(u)$ is a nondecreasing function satisfying $\lim_{u \searrow 0} \mathcal{H}_1(u)/u^h = 0$ and $\int_0^\infty \mathcal{H}_2(y)\, dy < \infty$ then

$$\begin{aligned} v^{(\kappa)} &= v^{(0)} \\ &- \sum_{k=1}^{h} \kappa^k \frac{1}{k!} \int_{\mathbb{R}^2} F_*^{(k)}(0; y)\, dy \mathrm{E}\Big[(I_\Phi(0))^k \Big] dy \\ &+ o(\kappa^h), \end{aligned}$$

  provided that the integrals are finite and

$$\mathrm{E}\big[\mathcal{H}_1\big(I_\Phi(0)\big) \big(I_\Phi(0)\big)^h \big] < \infty.$$

- *Similar approximations for moments of N_x ...*

A.4 Simulation of Model 3

In this section we briefly review results from [16] concerning (almost) exact simulation of Model 3.

A.4.1 Almost Exact Simulation of the Shot-Noise

In order to simulate cells of Model 3 with their exact distributions, one would have to know exact values of the shot-noise term I_ϕ which requires the simulation of the Poisson point process on the whole plane. This is infeasible, and instead, we use the following *almost exact simulation*: for a given size of *observation window* in which we want to simulate almost exactly our cells (say it is spherical observation window $B(0,R)$ of radius R), one selects a larger spherical *influence window* (say with a radius R') such that it is enough to take into account points of the point process in this larger influence window in order to get good estimate of the shot-noise term I_ϕ in the smaller observation window (and thus the shape of the cells) with high probability (see Figure 21). Formally one can prove that if the attenuation functions is of the form $l(x,y) < C/|x-y|^\beta$ for some constants $C > 0, \beta > 0$ and if the distribution of S has finite moment $E[S^{1/(\beta/2-\delta)}] < \infty$ for some $\delta \in [1, \beta/2]$, then one can show that for any $R, \varepsilon, \alpha > 0$, there exists $R' > 0$ such that

$$P\left(\sup_{|y|<R} \sum_{|X_i|>R'} S_i l(y, X_i) < \varepsilon\right) > 1 - \alpha\,. \tag{A.20}$$

Interesting cases where these assumptions are satisfied contain lognormal distribution of S.

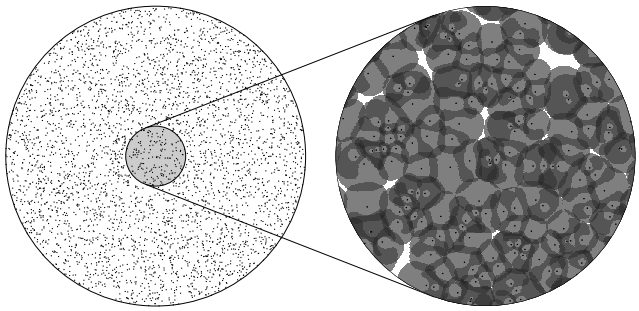

Figure 21: Almost exact simulation of Model 3 in the observation window $B(0,R)$, by taking into account the points of a larger influence window $B(0,R')$.

A.4.2 Conditional Simulation

The almost exact simulation of the shot-noise process allows one to get conditional distributions of the certain geometrical properties of the generic model. We will here again concentrate on Model 3.

Suppose two finite sets of points $z_1, \ldots, z_n$ and $z'_1, \ldots, z'_p$ in our observation window are given, and we want to perform an (almost) exact conditional simulation of Model 3, where the condition states that the points z_i are covered by *at least* n_i cells, and the points z'_i are covered by *at most* n'_i cells, for some given numbers $n_1, \ldots, n_n$ and $n'_1, \ldots, n'_p$. Note that this type

of conditions allows one to consider cases where the *exact number* of cells covering a point is specified.

The conditional simulator is meant for producing typical samples where these conditions are satisfied. Out of a sufficiently large set of these samples, one can then estimate various fine statistical properties of the geometry of the coverage process and in particular the contact distribution functions described in §4.

For this one can adapt, in the larger window, the so called backwards (coupling from the past) simulation of conditional coverage process developed for the Boolean model by Kendall [9].

The idea consists of two steps.

- First one constructs a Markov process $(\tilde{Z}_t)$ of patterns of points that has for stationary distribution the conditional distribution of Model 3. Points are generated at exponential periods (with an exponential distribution parameter equal to $\Lambda = \int_{B(0,R')} \lambda(x)\,dx$) and located in the window with distribution $\lambda(\cdot)/\Lambda$, but only *if their presence does not violate conditions of maximal coverage of the points* z_i'. Points located in the window stay there for exponential times (with parameter 1) and are removed, but only *if their absence does not violate the conditions of maximal coverage of the points* z_i'. If a particular removal would lead to the violation, then the point stays for another exponential time. One can show that the stationary distribution of this spatial birth-and-death process $(\tilde{Z}_t)$ is equal to the conditional distribution of Model 3 indeed.

- A long run simulation of this Marlov process, started from the empty window, gives random patterns with a distribution close to the conditional law of interest. The exact stationary distribution of the Markov process $(\tilde{Z}_t)$ can also be obtained in exact form, using *backwards* (*coupling from the past*) simulation [12] similar to these proposed by Kendall [9]. This method requires definition of two *extremal* processes of point patterns $(\tilde{Z}_t^{max})$, $(\tilde{Z}_t^{min})$ and an *order relation* $\prec$. These extremal processes are going to dominate (with respect to $\prec$) $(\tilde{Z}_t)$ for all $t \leq 0$ and if they coincide at $t = 0$, then $\tilde{Z}_0$ has the desired conditional distribution. The details can be found in [16].

Appendix B: Parameters of Case Studies

Here we summarize assumptions we made in the numerical examples throughout the whole paper.

B.1 Attenuation Function

For the attenuation, we assume one of the following two functions:

[A1] $l(x,y) = A(\max(|y-x|, r_0)^{-\alpha}$,

[A2] $l = (x,y)(1 + A|x-y|)^{-\alpha}$.

Note that both are modifications of *Hata's model*, in fact they only differ in the assumptions that are adopted in the neighborhood of the antenna.

B.2 Power

For antenna power we assume one of the following models.

[P1] P_i is constant,

[P2] P_i is exponential with mean $1/m$,

[P3] P_i is lognormal with parameters (ϵ, σ^2) meaning $P_i = 10^{(\epsilon+\sigma\xi)/10}$, where ξ is standard normal random variable. Note that ϵ, σ^2 can be interpreted as mean and variance of P_i expressed in dB.

B.3 Fading

If fading is assumed explicitly in a model we take it lognormal with its own parameters (ϵ, σ^2).

B.4 Fourier Transform of the Shot Noise

Direct computations show that under [A1] and [P2], in the homogeneous Poisson point process case, the Fourier transform of the shot noise $I_\Phi = I_\Phi(y)$ does not depend on y and is equal to

$$\begin{aligned}\psi_{I_\Phi}(\xi i) &= \mathrm{E}\left[e^{-i\xi I_\Phi}\right] \\ &= \exp\left[\lambda\pi\sqrt{\frac{iA\xi}{m}}\arctan\left(r_0^2\sqrt{\frac{m}{iA\xi}}\right) - \frac{\lambda}{2}\pi^2\sqrt{\frac{iA\xi}{m}}\right. \\ &\qquad \left. + \lambda\pi r_0^2\frac{r_0^4 - iA\xi - r_0^4 m}{iA\xi + r_0^4 m}\right],\end{aligned}$$

for $\xi \in \mathbb{R}$, where the branch of the complex square root function is chosen with positive real part (see [1]).

B.5 Cases

The following models are used for numerical illustration.

B.5.1 [Case 1]

(Parameters of Level-Sets for Shannon Capacity; cf. 3.1).

- attenuation as in [A1] with $A = 1, \alpha = 4, r_0 = 1$,
- homogeneous Poisson pattern of antennas, with intensity λ,
- power is as in [P2],
- $K = 1$,
- $\sigma^2 = 1$,
- κ, t as well as λ, m specified in particular examples.

This simple model allows for explicit calculations as we have an explicit expression for the Fourier transform of the corresponding shot noise.

B.5.2 [Case 2]

(Parameters of Level-Sets for Shannon Capacity; cf. 3.1) A more realistic model.

- attenuation as in [A1] with $A = 100, \alpha = 4, r_0 = 10$, with distance expressed in meters. It corresponds to a loss of about $140dB$ at 1000m,
- homogeneous Poisson pattern of antennas, with intensity λ,
- power as in [P3] with $\sigma = 8$,
- $K = 1$,
- $\sigma^2 = -1z69$ dBm/Hz $\times$ 1.25MHz $\approx 1.5 * 10^{-14}$W,
- $t = 0.34$,
- κ as well as λ, ϵ specified in particular examples.

B.5.3 [Case 3]

(Parameters of CDMA Downlink — Handoff Cells; cf. 3.2)

- attenuation as in [A1] with $A = 100, \alpha = 4, r_0 = 10$, with distance expressed in meters. It corresponds to a loss of about 140dB at 1000m,
- $\{X_i\}$ uniformly generated pattern of 64 points of BS's in the influence window $40 \times 40\text{km}^2$ which makes intensity $\lambda = 0.04\text{BS/km}^2$. The observation window is the inner square of size $20 \times 20\text{km}^2$.
- power as in [P3] with $P = 20$W,
- $\pi_i = p = 0.015$,
- Z_i lognormal with $\epsilon = 0$ and $\sigma^2 = 8$,
- $N_0 = -169$dBm/Hz,
- $W = 1.25$MHz,
- $T_i = 0.0025$.

B.5.4 [Case 4]

(Parameters of CDMA Downlink — Handoff Cells; cf. 3.2)

- attenuation as in [A2] with $A = 10, \alpha = 3$ with distance expressed in km. It corresponds to a loss of about 120dB at 1km,
- $N_0 = -169$dBm/Hz,
- $W = 1.25$MHz;
- power as in [P3] with $\epsilon = 7, \sigma^2 = (2.4)^2 = 5.76$, as suggested in [20],

- Z_i lognormal with $\epsilon = 0$ and $\sigma^2 = 8$,
- $T_i/\pi_i = 0.1$,
- $\lambda = 0.5$BS/km; if not specified otherwise figures bear on an observation window $[-5\text{km}, 5\text{km}]^2$ and are based on circular influence window with radius $R' = 40$km (cf. §A.4.2).

References

[1] Baccelli, F. and Błaszczyszyn, B. (2000), On a coverage process ranging from the Boolean model to the Poisson Voronoi tessellation, with applications to wireless communications. *INRIA report*, **4019**, to appear in *Adv. in Appl. Probab.*.

[2] Cover, T.M. and Thomas, J.A. (1991) *Elements of Information Theory*, J. Wiley & Sons, New York.

[3] Ehrenberger, U. and Leibnitz, K. (1999) Impact of clustered traffic distributions in CDMA radio network planning, in *Teletraffic Engineering in a Competitive World* by Key, P. and Smith, D. (editors) Elsevier, Amsterdam, 129–138.

[4] Gubner, J. (1996) Computation of shot-noise probability distributions and densities. *SIAM J. Comput.* **17**, 750–761.

[5] Gupta, P. and Kumar, P.R. (2000), The Capacity of Wireless Networks, IEEE Transactions on Information Theory, pp. 388-404, vol. IT-46, no. 2, March 2000.

[6] Hall, P. (1988), *Introduction to the Theory of Coverage Processes.* J. Wiley & Sons, New York.

[7] Heinrich, L. and Molchanov, I.S. (1994) Some limit theorems for extremal and union shot-noise processes. *Math. Nach.* **168**, 139–159.

[8] Heinrich, L. and Schmidt, V. (1985) Normal convergence of multidimensional shot noise and rates of this convergence. *Adv. in Appl. Probab.* **17**, 709–730.

[9] Kendall, W.S. and Thönnes, E. (1999), Perfect Simulation in Stochastic Geometry, *Pattern Recognition*, 32(9), pp. 1569-1586, special issue on random sets.

[10] Møller, J. *Lectures on random Voronoi tesselations*, volume 87 of *Lect. Notes in Statist.* Springer-Verlag, 1994.

[11] Prasad, R. and Ojanperä, T. (1998) An Overview of CDMA Evolution toward Wideband CDMA IEEE Communications Surveys, http://www.comsoc.org/pubs/surveys **1**, 2–29.

[12] Propp, J.G. and Wilson, D.B. (1996), Exact Sampling with Coupled Markov Chains and Applications to Statistical Mechanics, Random structures and Algorithms, Vol. 6, pp. 223-252.

[13] Rice, J. (1977) On a generalized shot noise. *Adv. in Appl. Probab.* **17**, 709–730.

[14] Rupf, M. and Massey, J.L. (1994) Optimum sequence multisets for synchronous code-division multiple-access channels, IEEE Transaction on Information Theory, **40**, 1261–1266.

[15] Stoyan, D., Kendall, W and Mecke, J. (1995) *Stochastic Geometry and its Applications*, John Wiley & Sons, Chichester.

[16] Tournois, F. Simulation of cells defined by the signal to interference ratio. In preparation.

[17] Veeravalli, V. and Sendonaris, A. (1999) The Coverage-Capacity Tradeoff in Cellular CDMA Systems." *IEEE Transactions on Vehicular Technology* **48** 1443–1451

[18] Viswanath, P. and Anantharam, V. (1999) Optimal Sequences and Sum Capacity of Synchronous CDMA Systems, IEEE Transaction on Information Theory, **45**, 1984–1991.

[19] Verdú, S. (1986) Capacity region of Gaussian CDMA channels: The symbol-synchronous case, Proc. 24th Allerton Conf., 1025-1034

[20] Viterbi, A. and Viterbi, A. (1993), Erlang Capacity of a Power Controlled CDMA System, IEEE On Selected Areas in Communications, pp. 892-900, vol. 11, no. 6, August 1993.

[21] Westcott, M. (1976) On the existence of a generalized shot-noise process. In Williams, E.J., editor, *Studies in Probability and Statistics. Papers in Honour of Edwin J.G. Pitman*, North-Holland, Amsterdam, pages 73–88.

Unité de recherche INRIA Rocquencourt
Domaine de Voluceau - Rocquencourt - B.P. 105 - 78153 Le Chesnay Cedex (France)

Unité de recherche INRIA Lorraine : Technopôle de Nancy-Brabois - Campus scientifique
615, rue du Jardin Botanique - B.P. 101 - 54602 Villers lès Nancy Cedex (France)
Unité de recherche INRIA Rennes : IRISA, Campus universitaire de Beaulieu - 35042 Rennes Cedex (France)
Unité de recherche INRIA Rhône-Alpes : 655, avenue de l'Europe - 38330 Montbonnot St Martin (France)
Unité de recherche INRIA Sophia Antipolis : 2004, route des Lucioles - B.P. 93 - 06902 Sophia Antipolis Cedex (France)

Éditeur
INRIA - Domaine de Voluceau - Rocquencourt, B.P. 105 - 78153 Le Chesnay Cedex (France)
http://www.inria.fr
ISSN 0249-6399